

Bottom water warming in the North Pacific Ocean

Masao Fukasawa¹, Howard Freeland², Ron Perkin², Tomowo Watanabe^{3*}, Hiroshi Uchida¹ & Ayako Nishina⁴

¹Ocean Observation and Research Department, Japan Marine Science and Technology Centre, Yokosuka, 237-0061, Japan

²The Institute of Ocean Sciences, Sidney, British Columbia, V8L 4B2, Canada

³Far-fisheries Laboratory, Japan Fisheries Agency, Shimizu, 424-8633, Japan

⁴Faculty of Fisheries, Kagoshima University, Kagoshima, 890-0056, Japan

* Present address: Central Fisheries Laboratory, Japan Fisheries Agency, Japan

Observations of changes in the properties of ocean waters have been restricted to surface¹ or intermediate-depth waters^{2,3}, because the detection of change in bottom water is extremely difficult owing to the small magnitude of the expected signals. Nevertheless, temporal changes in the properties of such deep waters across an ocean basin are of particular interest, as they can be used to constrain the transport of water at the bottom of the ocean and to detect changes in the global thermohaline circulation. Here we present a comparison of a trans-Pacific survey completed in 1985 (refs 4, 5) and its repetition in 1999 (ref. 6). We find that the deepest waters of the North Pacific Ocean have warmed significantly across the entire width of the ocean basin. Our observations imply that changes in water properties are now detectable in water masses that have long been insulated from heat exchange with the atmosphere.

Between 1991 and 1996 more than 100 hydrographic lines were surveyed to the highest standards then available. One such line scheduled for survey was designated World Ocean Circulation Experiment (WOCE) P1, across the subarctic Pacific. This line was not completed within the observation period for the WHP (WOCE Hydrographic Program) and had actually been completed in 1985. A revisit of P1 was scheduled as part of the Japanese Sub-Arctic Gyre Experiment and actually completed collaboratively between several Japanese agencies and the Institute of Ocean Sciences in Canada. Here we present results suggesting changes in the properties of the densest water in the North Pacific, which corresponds to the modified NADW (North Atlantic Deep Water) θ class water defined in the Samoa passage⁷.

The WHP line P01, located mainly along 47° N (see Fig. 1) from coast to coast, was surveyed in 1985 (refs 4, 5) and will be referred to

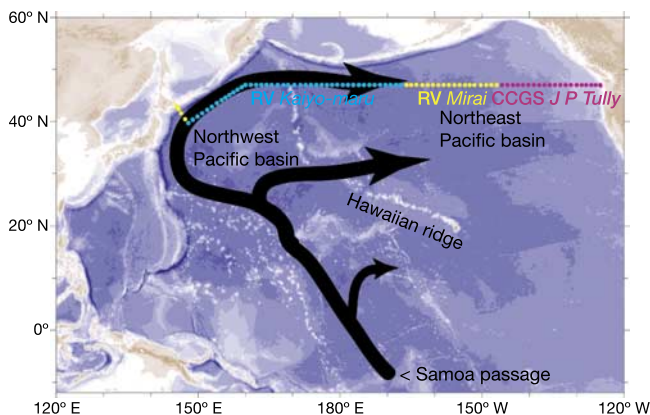


Figure 1 The location of stations occupied for WHP Line P1 revisit in 1999. The stations are colour-coded according to the ship completing that part of the survey. The dark arrows are adapted from ref. 17 to illustrate the dominant pathways by which bottom water from the Samoa passage is carried into the northeast Pacific basin.

here as P1_85. The P1 revisit (P1_99) was scheduled to examine the long-term variability in the subarctic Pacific⁶. The revisit survey was composed of four separate cruises. The accuracy of temperature and salinity measurement for the 1985 cruise is reported as 0.001 °C and 0.002 p.s.u. respectively⁴. Across the entire section in 1999, the accuracy of temperature (see Methods) and salinity measurement is better than 0.001 °C and about 0.001 p.s.u., respectively. We therefore consider differences smaller than 0.002 °C and 0.003 p.s.u. as being insignificant. These estimates are conservative and are thus more likely to discard real differences than to accept insignificant differences.

Figure 2a and b are cross-sections of the differences in temperature (ΔT) and salinity (ΔS) computed as 1999 conditions minus 1985 conditions. Regions of insignificant difference are not coloured. Below 3,000 m there is no area where the salinity differences are significant. Ignoring the shallower levels where differences due to seasonal variability are large, we note the following observations: (1) we see no obvious mismatches where the different sections of P1_99 are joined, suggesting that the difference significance levels truly are conservative. (2) Between 500 and 3,000 m there are large signals in both ΔT and ΔS that are negatively correlated with each other. (3) Below 5,000 m and extending to

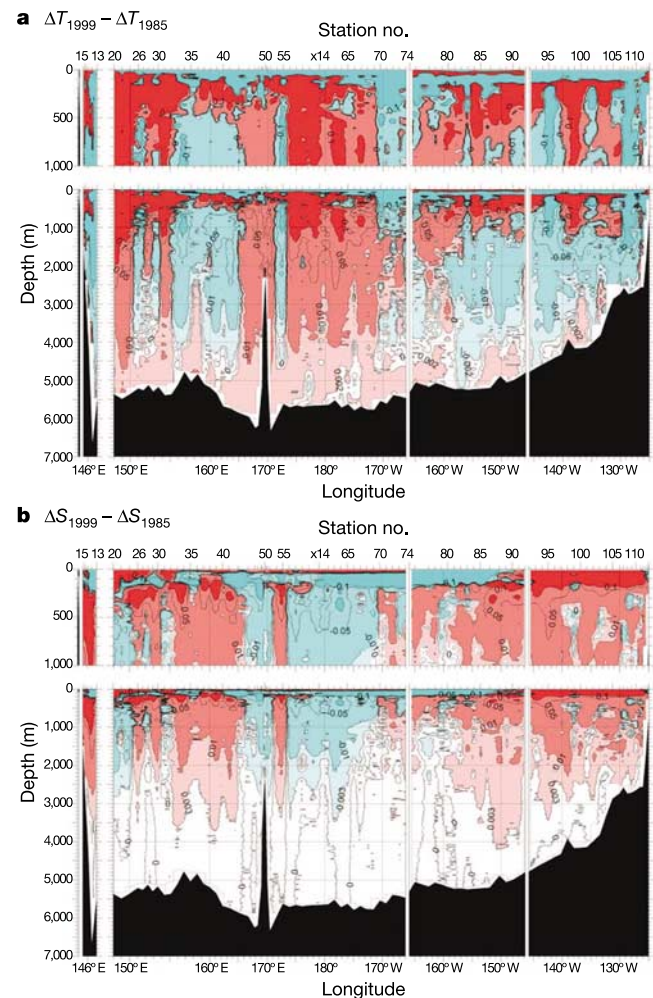


Figure 2 The difference in potential temperature (a) and salinity (b) between the two surveys of line P1 in 1999 and 1985, plotted against depth. The temperature and salinity differences are in °C and practical salinity units (p.s.u.), respectively. The contour intervals are variable and chosen to illuminate changes in the deeper waters. Dark red, very significant increases; pale red, less significant increases. Dark blue, very significant decreases; pale blue, less significant decreases.

the bottom there is a basin-wide warming of about 0.005 °C with no significant change in the salinity field.

Figure 3 shows ΔS again but plotted against longitude and the density variable σ_4 from values of 45.5 to the largest value observed in the section. The value $\sigma_4 = 45.5$ occurs at an average depth of about 1,400 m. We note that ΔS is larger in the Canadian part of this survey (from the CCGS *John P. Tully*), which might possibly be indicative of a lower quality of salinity determinations. However, nowhere in the section are the values of ΔS greater than our suggested detection limit of 0.003 p.s.u., further suggesting that our proposed detection limit is conservative. In the mid-depth region the values of ΔS are small compared with the values observed on pressure surfaces, suggesting that temperature and salinity changes are largely density-compensating. Thus these changes can largely be effected by a redistribution of water masses and do not require systematic changes in the properties of such water masses to be greater than 0.002 °C or 0.005 p.s.u..

In contrast, the changes below 5,000 m do not show the longitudinally banded structure that characterizes the mid-depth changes, and in particular show significant changes in temperature but not salinity. Thus these changes cannot be effected by vertical mass redistributions. Though the deep-water temperature changes are evident in all regions of the section the changes are particularly strong west of 160° W and especially near the Emperor seamount chain near 168° E. The deep and bottom waters of the North Pacific are filled with North Pacific Deep Water and modified North Atlantic Deep Water (mNADW), which composes the upper portion of the Lower Circumpolar Deep Water (LCDW). The NPDW and mNADW masses are characterized by potential temperatures lower than 2 °C and 1.2 °C, respectively, in the Samoan passage.

Figure 4 is constructed to clarify the changes taking place in the bottom water. For a series of potential temperature classes we compute a series of areas $A(\theta_i)$ defined as the total area along the section between $\theta_i - 0.005$ °C and $\theta_i + 0.005$ °C, then look at the difference field $\Delta A(\theta_i) = A_{1999}(\theta_i) - A_{1985}(\theta_i)$. The function $\Delta A(\theta_i)$ is plotted in the left panel of Fig. 4 and in the right panel we plot $I(\theta_k)$, where:

$$I(\theta_k) = \sum_{i=1}^k \Delta A(\theta_i)$$

and $i = 1$ denotes the coldest temperature bin. This clearly shows that the colder portion of the mNADW (that is, $\theta < 1.1$ °C) decreased its presence along 47° N between 1985 and 1999, whereas

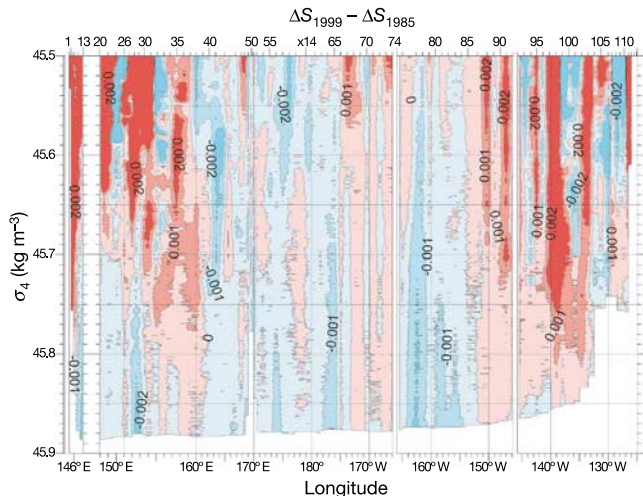


Figure 3 The difference in salinity between 1999 and 1985 for line P1, as in Fig. 2b, but plotted with the density parameter σ_4 as the vertical axis. σ_4 is a density anomaly referenced to a standard pressure of 4,000 decibar.

the warmer portion defined as 1.2 °C $\geq \theta \geq 1.1$ °C increased its presence. The integral from the bottom vanishes at 1.2 °C, showing that the total volume of mNADW has not changed. Throughout the NPDW mass the function $\Delta A(\theta_i)$ is close to zero, indicating no significant changes.

If we assume that 4×10^8 m² of the lower-area water (mean temperature 1.05 °C) is replaced by the upper-area water at a temperature of 1.15 °C, we can estimate a heat input of about 1.5×10^{14} J per metre width of the section. This is not a gigantic amount of heat. The temperature increase could be accommodated by increasing the heat input through the ocean bottom by about 0.080 W m⁻² west of 160° W. Sclater and Parsons⁸ review the mechanism of heat flow through the ocean bottom and show that the anticipated mean heat flow varies with the age of the crust, with the largest values being associated with very young crust near spreading ridges. Most of the WHP Section P1 is over very old oceanic crust with a mean heat flux of 0.042 W m⁻². This is close to estimates from hydrographic data⁹ of about 0.05 W m⁻². So, to accommodate the observed changes using geothermal heat input would require an increase above normal of almost 200% of the expected value. This is unlikely to have occurred and so we conclude that a large part of the warming must be explained by advective changes.

At depths where the warming was observed, vertical variations in salinity stratification are too small to detect any significant signal of a change in bottom water, however, dissolved oxygen shows a sharper stratification than salinity, providing an alternative view. Dissolved oxygen values analysed for the warmer portion (1.2 °C $\geq \theta \geq 1.1$ °C) and those for the colder portion (1.1 °C $\geq \theta$) were averaged zonally. Averaged dissolved oxygen values were determined to be 148 and 147 $\mu\text{mol kg}^{-1}$ for the warmer portion in P1_85 and P1_99, respectively. For the colder portion, we observe 158 and 157 $\mu\text{mol kg}^{-1}$ in P1_85 and P1_99, respectively. Thus, no significant change in the relationship between potential temperature and dissolved oxygen has occurred for either the warmer or colder portions of the mNADW. Again, it is unlikely that the observed warming can be explained by geothermal heating. We conclude therefore that the changes observed result from changes in the oceanographic circulation.

We have shown that the water in the densest water masses warmed along 47° N during the period 1985–1999 and conclude that a change in the oceanography is needed to account for this evolution. The warming was brought about by a decrease in the volume of the lower part of the mNADW at least along 47° N. The distribution of dissolved oxygen in the deep layers of the North

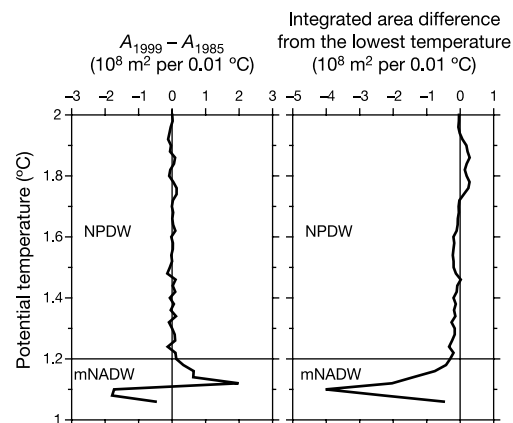


Figure 4 The difference in area between the 1999 and 1985 surveys in the areas along WHP Line P1 occupied by different potential temperatures. The bin size for potential temperature, used to define each area, is 0.01 °C. See text for full description of calculations and equations used.

Pacific¹⁰ suggests that the bottom water in the western North Pacific is fed from the Samoa passage, spreading northwards through the Wake Island passage (see Fig. 1). In the South Pacific, the source region of the bottom water in the North Pacific, warming of the NADW has previously been suggested^{7,11}, all reporting changes in water masses in the Samoa passage, within the relatively recent time period when data are available.

These suggest that there is significant variability in the supply of Antarctic Bottom Water. Another recent study¹² concluded that mid-depth Southern Ocean temperatures have warmed by as much as 0.17 °C since the 1950s, when the modern accumulation of hydrographic data in this area started, within the Antarctic Circumpolar Current. This warming, together with the warming trend of the global ocean¹ is naturally expected to affect the Antarctic overturning system. It is interesting to speculate whether or not the changes we observe are directly related to the changes being observed in the South Pacific, and this will presumably be answered only after further revisits of WHP lines in the Pacific Ocean. □

Methods

The 1999 surveys all used SeaBird 911 CTD systems and field calibrations were completed using Guildline salinometers. The temperature sensors on the Japanese systems were calibrated within a month before and after each cruise and the accuracy of the temperature measurement is known to be better than 0.0007 °C. The temperature sensor on the Canadian system was calibrated three weeks before the survey to 0.0006 °C. Salinity observations were corrected using the standard seawater batch correction. This involved corrections of -0.0014 and -0.0015 to the Japanese observations, and -0.0009 to the Canadian data. We note that the separate segments of the survey did not match in the deep water until these corrections were made. Before differences were computed between the 1985 and 1999 surveys we converted the 1985 temperature observations from the reported values in the IPTS68 temperature scale to ITS90 (ref. 13), and applied the standard seawater batch correction¹⁴⁻¹⁶, correcting salinities by +0.0012.

Received 22 July; accepted 31 December 2003; doi:10.1038/nature02337.

1. Levitus, S., Antonov, J. I., Boyer, T. P. & Stephens, C. Warming of the world ocean. *Science* **287**, 2225-2229 (2000).
2. Wong, A. P., Bindoff, N. L. & Church, J. A. Large-scale freshening of intermediate waters in the Pacific and Indian Oceans. *Nature* **400**, 440-443 (1999).
3. Roemmich, D. & Wunsch, C. Apparent changes in the climatic state of the deep North Atlantic Ocean. *Nature* **307**, 447-450 (1984).
4. Talley, L. D., Martin, M., Salameh, P. & the Oceanographic Data Facility. *Transpacific Section in the Subpolar Gyre (TPS47): Physical, Chemical, and CTD Data, R/V Thomas Thompson TT190, 4 August 1985-7 September 1985* 1-246 (Ref. 88-9, Scripps Inst. Of Oceanography, La Jolla, CA, 1988).
5. Talley, L. D., Joyce, T. & deSoeke, R. A. Trans-Pacific sections at 47°N and 152°W: distribution of properties. *Deep-Sea Res. (Suppl.)* **38**, S63-S82 (1991).
6. Uchida, H., Fukasawa, M. & Freeland, H. J. *WHP P01 Revisit Data Book 1-73* (Jamstec, Yokosuka, 2002).
7. Johnson, G. C., Rudnick, D. L. & Taft, B. A. Bottom water variability in the Samoa Passage. *J. Mar. Res.* **52**, 177-195 (1994).
8. Sclater, J. G. & Parsons, B. Oceans and continents: similarities and differences in the mechanisms of heat loss. *J. Geophys. Res.* **85**, 11535-11552 (1981).
9. Joyce, T. M., Warren, B. A. & Talley, L. D. The geothermal heating of the abyssal subarctic Pacific Ocean. *Deep-Sea Res.* **33**, 1003-1005 (1986).
10. Mantyla, A. & Reid, J. L. Abyssal characteristics of the world ocean waters. *Deep-Sea Res.* **30**, 805-833 (1983).
11. Johnson, G. C. & Orsi, A. H. Southwest Pacific water-mass exchanges between 1968/69 and 1990/91. *J. Clim.* **10**, 306-316 (1997).
12. Gille, S. H. Warming of the southern ocean since the 1950s. *Science* **295**, 1275-1277 (2002).
13. Preston-Thomas, H. The international temperature scale of 1990. *Metrologia* **27**, 3-10 (1990).
14. Mantyla, A. W. Standard seawater comparison updated. *J. Phys. Oceanogr.* **17**, 543-548 (1987).
15. Aoyama, M., Joyce, T., Kawano, T. & Takatsuki, Y. Standard seawater comparison up to P129. *Deep-Sea Res.* **49**, 1103-1114 (2002).
16. Kawano, T., Takatsuki, Y., Imai, J. & Aoyama, M. Seawater and quality evaluation of the standard seawater supplied in a bottle. [In Japanese with English abstract]. *J. Jpn Soc. Mar. Surv. Tech.* **13**, 11-18 (2001).
17. Reid, J. L. On the total geostrophic circulation of the Pacific Ocean: flow patterns, tracers and transports. *Prog. Oceanogr.* **39**, 263-352 (1997).

Acknowledgements We thank the officers and crew of the three research vessels (RV *Kaiyo-maru* of JFA, RV *Mirai* of JAMSTEC, and CCGS *John P. Tully*) and all technical assistants. The Canadian contribution was funded by the Strategic Science Fund of the Department of Fisheries and Oceans, and the Japanese contributions were funded by the Promotional Foundation for Science and Technology of the Science and Technology Agency of Japan (now known as the Ministry of Education, Culture, Sports, Science and Technology).

Competing interests statement The authors declare that they have no competing financial interests.

Correspondence and requests for materials should be addressed to M.F. (fks@jamstec.go.jp) or H.F. (FreelandHj@pac.dfo-mpo.gc.ca).

Rejuvenation of the lithosphere by the Hawaiian plume

Xueqing Li¹, Rainer Kind^{1,2}, Xiaohui Yuan¹, Ingo Wölbern¹ & Winfried Hanka¹

¹GeoForschungsZentrum Potsdam, Telegrafenberg, 14473 Potsdam, Germany
²Freie Universität Berlin, FR Geophysik, Malteserstrasse 74-100, 12249 Berlin, Germany

The volcanism responsible for creating the chain of the Hawaiian islands and seamounts is believed to mark the passage of the oceanic lithosphere over a mantle plume^{1,2}. In this picture hot material rises from great depth within a fixed narrow conduit to the surface, penetrating the moving lithosphere³. Although a number of models describe possible plume-lithosphere interactions⁴, seismic imaging techniques have not had sufficient resolution to distinguish between them. Here we apply the S-wave 'receiver function' technique to data of three permanent seismic broadband stations on the Hawaiian islands, to map the thickness of the underlying lithosphere. We find that under Big Island the lithosphere is 100-110 km thick, as expected for an oceanic plate 90-100 million years old that is not modified by a plume. But the lithosphere thins gradually along the island chain to about 50-60 km below Kauai. The width of the thinning is about 300 km. In this zone, well within the larger-scale topographic swell, we infer that the rejuvenation model⁵ (where the plume thins the lithosphere) is operative; however, the larger-scale topographic swell is probably supported dynamically.

Thermomechanical processes caused by plume-lithosphere interactions have been studied for several decades. Various models have been proposed to explain the generating mechanism of the Hawaiian swell: (1) a model in which the dynamic pressure of the plume material flowing in the asthenosphere away from the plume centre supports the uplift of the sea floor^{4,6}; (2) the thermal resetting (rejuvenation) model, in which the oceanic lithosphere is heated when it passes the hotspot, and thinning of the lithosphere causes isostatic uplift of the Hawaiian swell⁵; (3) a model in which

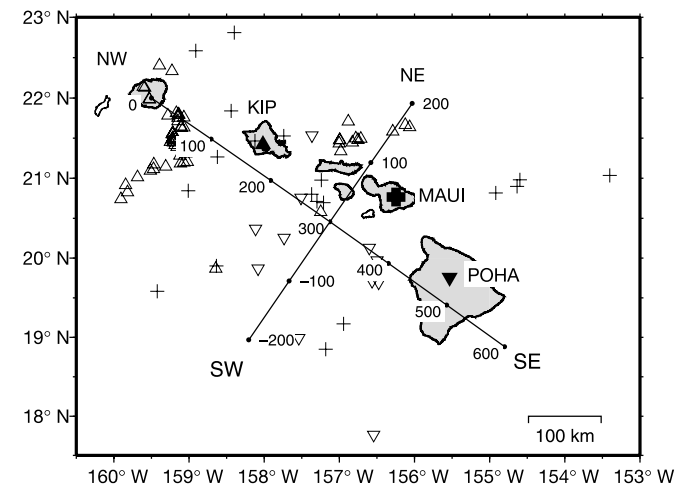


Figure 1 Location map of permanent broadband stations KIP (IRIS/GEOSCOPE), MAUI (GEOFON) and POHA (IRIS/USGS). Piercing points of S-receiver functions at 100 km depth are shown (same symbols as stations). Two lines labelled NW-SE and SW-NE indicate the two sections shown in Fig. 2 onto which the S-receiver functions are projected. Section NW-SE is along the island chain while section SW-NE is perpendicular to the chain.